Porous 3-D honeycomb architecture by self-assembly of helical H-bonded molecular tapes†

Arnaud-Pierre Schaffner,[‡a] Gersande Lena,[a] Solveig Roussel,[§a] Anne Wawrezinieck,[ab] André Aubry,[c] Jean-Paul Briand,[a] Claude Didierjean*[c] and Gilles Guichard*[a]

Received (in Cambridge, UK) 3rd April 2006, Accepted 16th August 2006
First published as an Advance Article on the web 11th September 2006
DOI: 10.1039/b604747e

Enantiopure dipeptide-derived 1,3,5-triazepan-2,6-diones 1a and 1c form H-bonded *3_1* helical molecular tapes with *P* chirality in the solid state; in the case of 1a, these columnar tapes self-assemble through aromatic–aromatic interactions to give hollow tubular structures.

The current interest in the formation of hollow tubular structures by controlled self-organization or self-assembly of organic units stems from the possibilities of generating molecules (*i.e.* ion channels, pores) with function (*e.g.* antibacterial agents,[1] "organic zeolites",[2] sensors[3]). Several strategies have been reported to convert synthetic peptide-based materials into bio-inspired tubular supramolecular assemblies. These include hollow β-helices from D,L-peptides,[4,5] barrel-hoop motifs from stacked macrocyclic peptides,[1,6] barrel-stave motifs from rigid-rod peptide conjugates,[3,8] helical pores from dipeptides[8] and dendritic dipeptides.[9] Herein we report the formation of helical molecular tapes and helical tubular structures self-assembled in bulk from dipeptide-derived heterocycle **1** (Scheme 1).

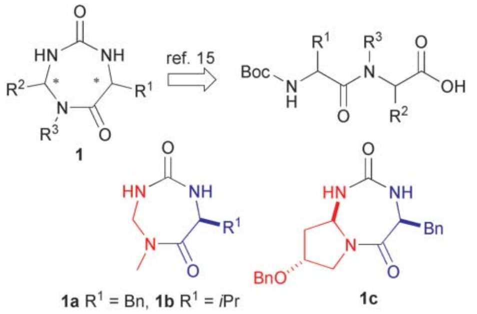

Scheme 1 Solution phase synthesis of 1,3,5-triazepan-2,6-diones. (a) EtOCOCl, NMM, THF, −20 °C, then NaN_3 in H_2O; (b) Toluene, 65 °C, then HOSu and pyridine; (c) TFA, 30 min; (d) DIPEA, MeCN; (e) PS-DIPEA, CH_2Cl_2.

H-Bonded tapes created by formation of $R\binom{2}{2}8$ dimers between cyclic secondary diamide units (either fused (*e.g.* cyclic ureas), directly joined or separated by one (*e.g.* 2,5-diketopiperazines) or more than one atom) are important motifs in the field of organic molecular crystals because of their simplicity, their robustness and their predictability.[10] Most cyclic diamides studied have planar or nearly planar structures and since NH donors show a statistical preference to approach in the plane of the C=O group,[11] the resulting aggregate is usually planar or two-dimensional. In molecules where the two amide groups are not coplanar, the tape motif generally tends to buckle.[12] Formation of non-planar cyclic hexamers has been documented for non-planar bicyclic diacylaminals.[14]

We recently reported the development and some applications of the 1,3,5-triazepan-2,6-dione scaffold **1** (Scheme 1).[14] Preliminary X-ray structure analysis of representative members ($R^2 \neq H$) revealed a markedly folded conformation (angle (α) between amide and urea planes ~120°) as well as a tendency to form $R\binom{2}{2}8$ dimers of type I (Fig. 1).[14,15] These observations suggested to us that triazepandiones **1**, depending on the pattern of R^1–R^3 substituents and subject to the participation of N^1H in the formation of $R\binom{2}{2}8$ dimers (type I′ or II), could eventually pack into non-planar (*e.g.* helical) H-bonded tapes relevant to the elaboration of diverse and complex supramolecular architectures.

Enantiopure cyclic ureas **1a** and **1c** (Scheme 1) were both prepared in 72% overall yield from dipeptides Boc-L-Phe-Sar-OH and Boc-L-Phe-L-Hyp(Bn)-OH, respectively.[14] **1a** crystallized from 1,4-dioxane in the hexagonal $P6_1$ space group with one molecule in the asymmetric unit. Crystals of compound **1c**, obtained by slow evaporation of a mixture of dichloromethane and iPr_2O, exhibit the monoclinic $P2_1$ space group with three independent molecules in the asymmetric unit.¶ As expected, the ring in **1a** and **1c** adopts a folded conformation (α = 120.7° and 121.2° in **1a** and **1c**

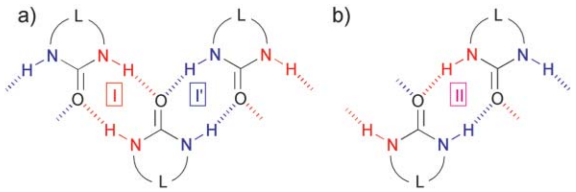

Fig. 1 Schematic representation of the two putative H-bonded tape motifs that can be formed between cyclic ureas **1** (a) from alternating type I and type I′ $R\binom{2}{2}8$ dimers and (b) from hybrid type II $R\binom{2}{2}8$ dimers. L represents the linking portion between the two urea nitrogens.

---

[a] *Immunologie et Chimie Thérapeutiques (ICT), UPR CNRS 9021, Institut de Biologie Moléculaire et Cellulaire, 15 rue Descartes, F-67084 Strasbourg, France. E-mail: g.guichard@ibmc.u-strasbg.fr; Fax: +33 3 88 61 06 80; Tel: +33 3 88 41 70 25*
[b] *Institut Charles Sadron, UPR CNRS 22, 6 rue Boussingault, BP 40016, F-67083 Strasbourg Cedex, France*
[c] *LCM3B, UMR-CNRS 7036, Groupe Biocristallographie, Université Henri Poincaré, BP 239, 54506 Vandoeuvre, France. E-mail: Claude.Didierjean@lcm3b.uhp-nancy.fr*

† Electronic supplementary information (ESI) available: Structural and spectral data (Fig. S1–S5). See DOI: 10.1039/b604747e

‡ *Present address*: EMC microcollections GmbH, D-72070 Tübingen, Germany.

§ *Present address*: Diverchim, Les Marches de l'Oise, 100 rue Louis Blanc, F-60765 Montataire, France.

respectively) with side chains occupying pseudoequatorial positions. The main structural feature is that both **1a** and **1c** crystallize as *3_1* helical molecular tapes with *P* chirality (Fig. 2). In the structure of **1c**, the *3_1* is a non-crystallographic axis, with only the seven-membered ring and the Phe side chain following the symmetry law (Fig. 2b). $R\binom{2}{2}8$ dimers in the helical tape motif are identical to type II (Fig. 1), that is they are assembled from two chemically distinct NH donors – *i.e.* N^1H on one molecule and N^3H on another. In both **1a** and **1c**, the N^3–H···O=C (D = 2.84 Å in **1a**) bond forming the hybrid dimer is systematically shorter than the corresponding N^1–H···O=C (D = 3.04 Å in **1a**), thus suggesting that N^1H is a better H-bond donor. If both N–H···O=C H-bonds in these hybrid $R\binom{2}{2}8$ dimers form in approximately the direction of the oxygen sp^2 lone pairs (in **1a**: ϕ_H = 30° and 26° for N^3–H···O=C and N^1–H···O=C, respectively),[16] the *3_1*-helicoidal arrangement, however, imposes the H-bond geometry to deviate from planarity (in **1a**: θ_H = 48° and 56° for N^3–H···O=C and N^1–H···O=C, respectively).[12] In the crystal structure of **1c** the *3_1*-tape motif is reinforced by a water molecule which bridges with the C=O amide of one molecule and the OBn oxygen of a molecule identical by translation.

In both molecules, (*P*)-*3_1* columnar tapes self-assemble parallel to their helix axis through extensive aromatic–aromatic interactions. In the structure of **1a**, the C=O amide forms a weak H-bond with one of the two tetrahedral carbons of the seven-membered ring (D = 3.42 Å, d = 2.53 Å and θ = 153°). The columnar tapes form the boundaries of channels. These are centred on and run parallel to the hexagonal axis of the crystal of **1a** (Fig. 3a and 3b) and are defined by a right-handed *6_1* helical arrangement of heterocyclic rings (Fig. 3c). Although difference map analysis revealed empty pores in the crystal, the channels with an average internal diameter of 6.1 Å were found to be large enough to accommodate solvent molecules. The change of crystallization solvent from 1,4-dioxane to 1,4-dioxane–iPr_2O or dichloromethane–iPr_2O solutions did not affect the tubular architecture but electron density inside the tubular cavities of these crystals was interpreted as disordered solvent (iPr_2O) molecules. This was supported by ^1H-NMR analysis of a $CDCl_3$ solution of air-dried crystals of **1a** grown from dichloromethane–iPr_2O solution which indicated a composition of **1a**·1/6 iPr_2O. To gain insight into the dynamics of guest solvent molecules inside the pores, several data sets were collected for crystals of **1a** grown from dioxane–iPr_2O after drying under vacuum at room temperature or after heating (308, 318, 358 K) for 48 h. In all cases, modification of the cell dimensions, overall geometry and electron density inside the pores was negligible (Fig. 1 of the ESI†).¶ The thermal stability of the solvent molecules was further investigated by thermogravimetric analysis (TGA). TGA experiments (Fig. 2 of the ESI†) show a weight loss of 9.5% in the temperature range 80–195 °C which is consistent with the loss of *ca.* ¼ molecule of iPr_2O. Further evidence for tubular self-aggregation of **1a** in bulk came from TEM imaging (Fig. 4; see also Fig. 3 of the ESI†) which revealed the formation of relatively straight polydisperse nanorods with thickness $\leqslant$ 20 nm.[17]

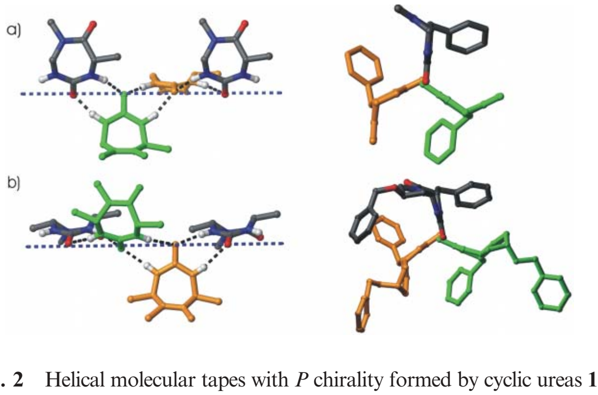

Fig. 2 Helical molecular tapes with *P* chirality formed by cyclic ureas **1a** (a) and **1c** (b) viewed along and top-down their axis respectively. The side chains have been omitted from the left diagram and the hydrogens have been omitted from the right diagram for clarity.

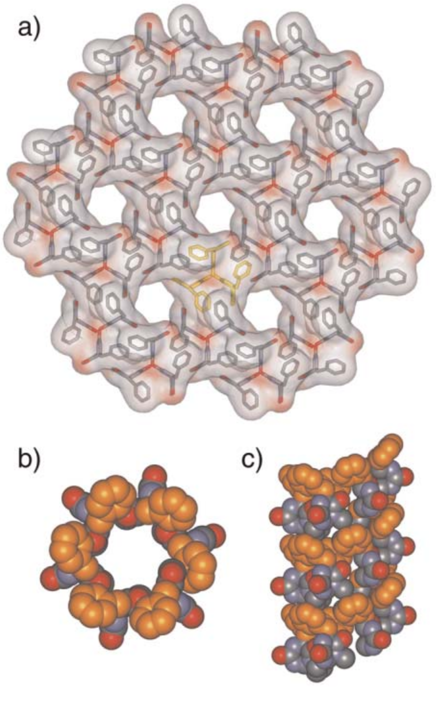

Fig. 3 Packing of (*P*)-*3_1* molecular tapes parallel to their helix axis in **1a** results in the formation of 3-D honeycomb type architecture with an internal van der Waals diameter of the pores of 6.1 Å.

In contrast, **1c** does not exhibit any tubular structure. Although the large Hyp(Bn) side chain does not prevent the formation of (*P*)-*3_1* molecular tapes, it prevents the formation of the large pores in the crystal. It is worth mentioning that the molecular packing preserved along the (*P*)-*3_1* axis is also maintained along a perpendicular direction. Thus, two of the three independent aromatic rings of the Phe side chain exhibit the same edge-to-face aromatic interaction as that observed in the crystal structure of **1a**

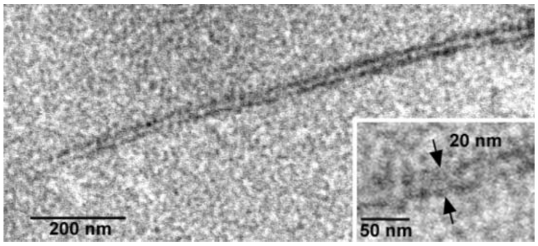

Fig. 4 TEM negative stain imaging of **1a**.

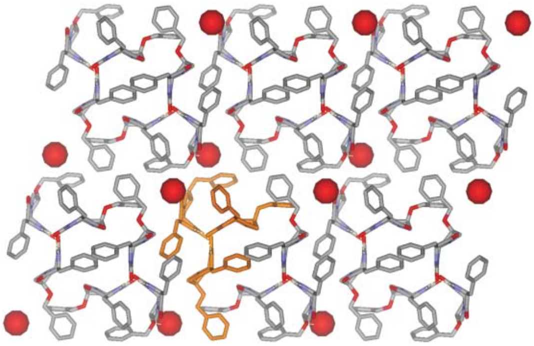

Fig. 5 Packing of columnar tapes in **1c** parallel to their helix axis. For clarity, one helical tape is shown in orange.

(compare Fig. 5 and Fig. 3a). This observation underscores the possible role of the Phe side chain in the building of the helical H-bonded molecular tapes. This is further supported by the finding that **1b**[18] which lacks an aromatic R^1 side chain does not form helicoidal molecular tape in the solid state but a complex two-dimensional layer involving $R(^{2}_{2})_8$ dimers of type I′ (data not shown).

The easy synthesis of the 1,3,5-triazepan-2,6-dione skeleton from a large variety of dipeptides[14] opens up interesting possibilities to study the factors that govern the formation of such helical H-bonded networks in the crystals of compounds **1** as well as the generality of this tape motif. The possibility of creating other supramolecular architectures using helical molecular tapes will be addressed in future development of this work.

The authors thank Yves Guilbert for running TGA experiments, Marion Decossas for help with TEM imaging as well as Alexandre Bouché and Emmanuel Wenger for X-ray diffraction experiments. This research was supported in part by the Centre National de la Recherche Scientifique (CNRS) and ImmuPharma. A CIFRE fellowship from ImmuPharma and ANRT for GL is gratefully acknowledged.

Notes and references

¶ **Crystal data of 1a**: $C_{12}H_{15}N_3O_2$, $M = 233.27$: prismatic crystals grown by slow evaporation of dioxane, crystal size 0.3 × 0.3 × 0.1 mm^3, hexagonal, $a = 15.583(2)$, $c = 9.964(1)$ Å, $U = 2095.4(4)$ Å^3, $T = 293$ K, space group $P6_1$ (no. 169), $Z = 6$, μ(Cu-Kα) = 0.634 mm^{-1}, 1380 reflections measured which were used in all calculations. The absolute stereochemistry of **1a** is based on the known configuration of Boc-L-Phe-Sar-OH. The positions of the H atoms attached to N atoms were located from a difference map and the N–H bond distance was restrained to a value of 1.03(1) Å (ref. 19). H atoms connected to carbon were placed at calculated positions using a riding model. The final $R(F_2)$ was 0.0462 for 1302 reflections with $I > 2\sigma(I)$.

Crystal data of 1a solvate: $C_{12}H_{15}N_3O_2 \cdot x iPr_2O$: prismatic crystals grown by slow evaporation of dioxane–iPr$_2$O and heated at 358 K for 48 h, crystal size 0.6 × 0.6 × 0.2 mm^3, hexagonal, $a = 15.3543(11)$, $c = 9.7571(17)$ Å, $U = 1992.1(4)$ Å^3, $T = 100$ K, space group $P6_1$ (no. 169), $Z = 6$, μ(Mo-Kα) = 0.082 mm^{-1}, 18031 reflections measured ($R_{int} = 0.063$). The absolute stereochemistry of **1a** is based on the known configuration of Boc-Phe-Sar-OH. Once the model is refined, the difference map exhibits positive electron density peaks which are larger than expected. These peaks are located inside the channels and they can be attributed to disordered solvent. It has not been possible to build a correct model of the solvent inside the cavities. All H atoms were placed at calculated postions. The final $R(F_2)$ was 0.0636 for 1217 reflections with $I > 2\sigma(I)$.

Crystal data of 1c hydrate: $C_{21}H_{23}N_3O_3 \cdot 0.76H_2O$, $M = 370.05$: prismatic crystals grown by slow evaporation of CH$_2$Cl$_2$–iPr$_2$O, crystal size 0.2 × 0.1 × 0.1 mm^3, monoclinic, $a = 15.7533(3)$, $b = 10.5328(2)$, $c = 17.8744(5)$ Å, $\beta = 102.8050(10)°$, $U = 2892.07(11)$ Å^3, $T = 293$ K, space group $P2_1$ (no. 4), $Z = 6$, μ(Mo-Kα) = 0.087 mm^{-1}, 27853 reflections measured ($R_{int} = 0.047$). The absolute stereochemistry of **1a** is based on the known configuration of Boc-L-Phe-L-Hyp(Bn)-OH. In the three independent molecules, the benzene group of the Hyp(Bn) residue is disordered. The aromatic bond distance was restrained to 1.39(1) Å. In one molecule, the methylbenzene group of the Hyp(Bn) residue was modeled over two positions and additional restraints were applied: the aromatic rings were restrained to be approximately planar; the distances of the ether bond and the C_{sp^3}–$C_{aromatic}$ bond were restrained to 1.44(1) Å and 1.51(1) Å, respectively; a common isotropic displacement parameter was applied to atoms of each methylbenzene group. The relative occupancies were refined and converged to 0.53(1) : 0.47(1). Compound **1a** crystallizes with one water molecule in an asymmetric unit, the water molecule site is not fully occupied and has been refined with a site-occupancy factor of 0.76(1). All H atoms were placed at calculated positions. The final $R(F_2)$ was 0.0532 for 2781 reflections with $I > 2\sigma(I)$.

CCDC 603581, 603582 and 617812. For crystallographic data in CIF or other electronic format see DOI: 10.1039/b604747e

1 S. Fernandez-Lopez, H. S. Kim, E. C. Choi, M. Delgado, J. R. Granja, A. Khasanov, K. Kraehenbuehl, G. Long, D. A. Weinberger, K. M. Wilcoxen and M. R. Ghadiri, *Nature*, 2001, **412**, 452.
2 J. Yang, M. B. Dewal and L. S. Shimizu, *J. Am. Chem. Soc.*, 2006, **128**, 8122.
3 G. Das and S. Matile, *Chem.–Eur. J.*, 2006, **12**, 2936.
4 E. Benedetti, B. Di Blasio, C. Pedone, G. P. Lorenzi, L. Tomasic and V. Gramlich, *Nature*, 1979, **282**, 630.
5 H. D. Arndt, D. Bockelmann, A. Knoll, S. Lamberth, C. Griesinger and U. Koert, *Angew. Chem., Int. Ed.*, 2002, **41**, 4062.
6 D. T. Bong, T. D. Clark, J. R. Granja and M. R. Ghadiri, *Angew. Chem., Int. Ed.*, 2001, **40**, 988.
7 N. Sakai and S. Matile, *Chem. Commun.*, 2003, 2514.
8 C. H. Görbitz, M. Nilsen, K. Szeto and L. W. Tangen, *Chem. Commun.*, 2005, 4288.
9 V. Percec, A. E. Dulcey, V. S. Balagurusamy, Y. Miura, J. Smidrkal, M. Peterca, S. Nummelin, U. Edlund, S. D. Hudson, P. A. Heiney, H. Duan, S. N. Magonov and S. A. Vinogradov, *Nature*, 2004, **430**, 764.
10 J. C. MacDonald and G. M. Whitesides, *Chem. Rev.*, 1994, **94**, 3523.
11 R. Taylor, O. Kennard and W. Versichel, *J. Am. Chem. Soc.*, 1983, **105**, 5761.
12 D. N. White and J. D. Dunitz, *Isr. J. Chem.*, 1972, **10**, 249.
13 R. B. Grossman, K. Hattori, S. Parkin, B. O. Patrick and M. A. Varner, *J. Am. Chem. Soc.*, 2002, **124**, 13686.
14 G. Lena, E. Lallemand, A. Charlotte Grüner, J. Boeglin, S. Roussel, A.-P. Schaffner, A. Aubry, J.-F. Franetich, D. Mazier, I. Landau, J.-P. Briand, C. Didierjean, L. Rénia and G. Guichard, *Chem.–Eur. J.*, 2006, DOI: 10.1002/chem.200600560.
15 G. Lena, E. Wenger, G. Guichard and C. Didierjean, *Acta Crystallogr., Sect. E*, 2006, **62**, o518.
16 For the definition of ϕ_H and θ_H see ref. 12.
17 The aggregation of **1a** was also investigated in solution and in the gas phase. NMR spectroscopy studies of **1a** in CDCl$_3$ revealed concentration-dependent changes in the chemical shifts of N^{3}H (1.91 ppm between 0.14 mM and 143 mM) and N^{1}H to a lesser extent (0.54 ppm over the same range of concentration), thus suggesting the participation of both NHs in H-bonding possibly *via* the formation of $R(^{2}_{2})8$ dimers. In dioxane-d_8, N^{1}H and N^{3}H showed a very similar chemical shift variation (0.6 and 0.4 ppm, respectively between 1.6 mM and 81 mM). The formation of dimers and higher order aggregates of **1a** in solution was further supported by studies in the gas phase. Dimeric [2M + H$^+$] plus [2M + Na$^+$] (51% composition) and trimeric [3M + H$^+$] (5.3% composition) ions were observed in electrospray ionization mass spectrometry (ESI-MS) spectra of **1a** (Figs. 4–6 in ESI).
18 Compound **1b** was prepared in 63% yield from dipeptide Boc-L-Val-Sar-OH as described in ref. 15.
19 R. Taylor and O. Kennard, *Acta Crystallogr., Sect. B*, 1983, **39**, 133.